Thermochimica Acta, 165 (1990) 73–83
Elsevier Science Publishers B.V., Amsterdam

THE REDUCTION OF V_2O_5. PART I. REDUCTION BY CARBON MONOXIDE

F. STANDER

Council for Mineral Technology, Private Bag X3015, Randburg 2125 (South Africa)

C.P.J. VAN VUUREN *

Department of Materials Science and Metallurgical Engineering, University of Pretoria, Pretoria 0002 (South Africa)

(Received 21 December 1989)

ABSTRACT

The reduction of V_2O_5 by CO was studied using thermal analysis, X-ray powder diffraction, and electron and optical microscopy. It was shown that the reduction reaction passes through the oxide phases V_6O_{13} and VO_2 with V_2O_3 being the final product. The kinetics of the reduction seems to be described by the Avrami–Erofe'ev equation with $n = 4$ for V_2O_5 powder and $n = 2$ for the platelets. The reaction starts on the surface of the crystal and proceeds towards the centre.

INTRODUCTION

Vanadium oxides have wide industrial applications such as the vanadium oxide based catalysts which are used in a number of oxidation processes [1–3]. There seem, however, to be uncertainties about the stoichiometry of the various intermediate oxides which form during the reduction reaction of V_2O_5. Stringer constructed a phase diagram of the vanadium–oxygen system after a critical literature review of the vanadium oxides and suggested the existence of 12 oxide phases in the composition range V_2O_5–V_2O_3 [4]. Recently, Pospisil studied the reduction of Ni–V_2O_5 with H_2 and found that various intermediate oxides are formed during the course of the reaction [5]. Bosch et al. studied the reduction of V_2O_5 with H_2 using the temperature-programmed reaction (TPR) technique and found evidence for the formation of V_6O_{13}, VO_2 and V_2O_3 [6]. They suggested that the oxide V_6O_{11} could form as an intermediate, but could not find evidence for its existence.

* Author to whom correspondence should be addressed.

0040-6031/90/$03.50

In view of these uncertainties surrounding the various oxide phases which form as intermediates, a study was conducted to determine the stoichiometry of the intermediate oxides which form during the reduction of V_2O_5 by CO and H_2. This paper describes the results obtained from a study of the reduction of V_2O_5 with CO.

EXPERIMENTAL

Materials

The V_2O_5 (99.6% pure) powder used was obtained from J.T. Baker Chemical Co. Large orange V_2O_5 crystals were prepared by decomposition of ammonium metavanadate in air at 700 °C for 2 h, followed by slow cooling of the V_2O_5 melt in the furnace.

Thermal analysis

A Stanton Redcroft STA 780 simultaneous thermal analyser was used to collect the dynamic and isothermal TG data. The apparatus and method of data collection have been previously described [7,8]. DTA studies were carried out on a Perkin–Elmer DTA 1700 differential thermal analyser which was controlled by a System 7/4 thermal analysis controller and 3700 Data Station. A dynamic atmosphere of CO (99% pure) at a flow rate of 50 $cm^3\ min^{-1}$ was used for all experiments.

Isothermal TG data for kinetic analysis were collected in the temperature range 380–600 °C. The method of calculation was as described previously [8].

X-ray powder diffraction

XRPD analysis was used to identify the intermediate and final products during the reduction process. A Seifert MZ IV instrument with Cu $K\alpha$ radiation was used. The ASTM Powder Diffraction Files of the JCPDS were used as reference for the characterisation of the vanadium oxides.

Electron microscopy

A Philips P500 scanning electron microscope was used to study the partly reduced samples.

RESULTS AND DISCUSSION

The morphology of the different V_2O_5 crystal types used is shown in Fig. 1. The powder consisted of agglomerates of poorly defined crystallites with a surface area of 2.87 ± 0.02 m^2 g^{-1}. The platelets consisted of well developed crystals with the largest face corresponding to the (010) face. The average surface areas were found to be < 0.5 m^2 g^{-1} for crystals passing through a 250 μm sieve.

Dynamic thermal analysis

The TG and DTA curves for the reduction of the V_2O_5 powder are given in Figs. 2A and 2B respectively. At a heating rate of 5 °C min^{-1}, only a single exothermic reaction step is visible in the temperature range 540–720 °C. The 17.0% mass loss observed is in fair agreement with the calculated value of 17.59% for the reduction of V_2O_5 to V_2O_3. X-ray powder

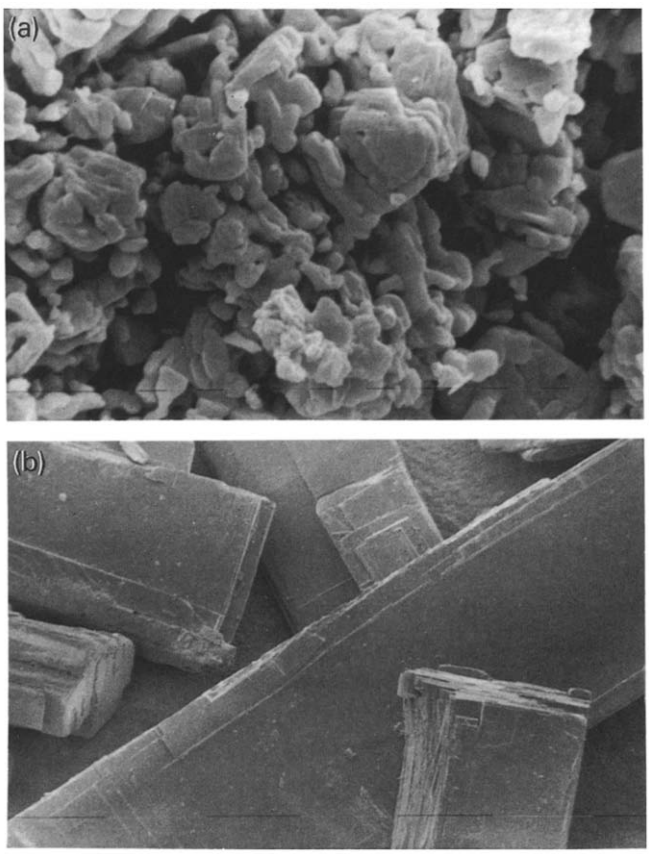

Fig. 1. Morphology of the different V_2O_5 crystal types used: a, powder sample; b, platelets.

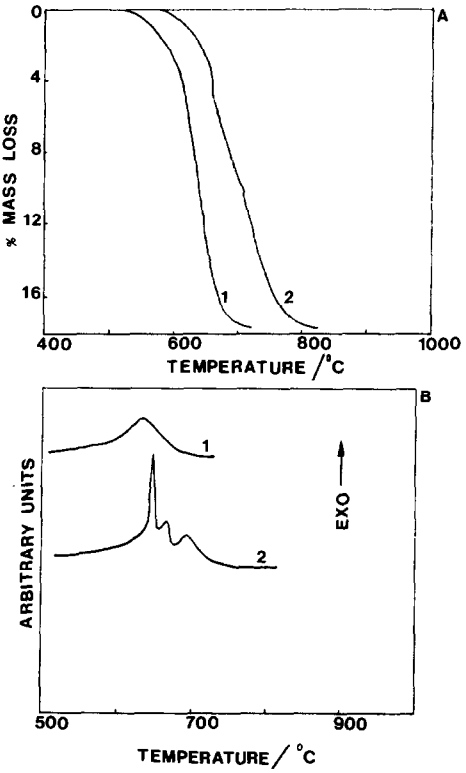

Fig. 2. Thermogravimetric (A) and DTA (B) curves of the reduction of V_2O_5 powder by CO at different heating rates: curve 1, 5 °C min^{-1}; curve 2, 10 °C min^{-1}.

diffraction, see Table 1, confirmed that the final product was V_2O_3. At the higher heating rate of 10 °C min^{-1}, the reaction temperature range shifted towards higher temperatures and three overlapping exothermic reactions

TABLE 1

X-ray powder diffraction lines (d-spacings (Å) with relative intensities in parentheses) as observed for the various intermediate oxides which form during the reduction of V_2O_5 by CO (only the eight strongest lines are listed)

V_6O_{13}		VO_2		V_2O_3	
Obs.	ASTM	Obs.	ASTM	Obs.	ASTM
5.88 (40)	5.76 (40)	3.31 (20)	3.31 (30)	3.65 (70)	3.65 (60)
4.99 (50)	4.98 (20)	3.22 (100)	3.20 (100)	2.71 (90)	2.70 (80)
3.52 (90)	3.51 (100)	2.66 (10)	2.68 (30)	2.45 (70)	2.47 (60)
3.33 (100)	3.32 (80)	2.43 (20)	2.43 (60)	2.19 (40)	2.19 (20)
2.97 (40)	2.96 (60)	2.14 (15)	2.14 (50)	1.83 (25)	1.83 (25)
2.68 (30)	2.67 (80)	1.66 (25)	1.66 (20)	1.70 (100)	1.69 (100)
1.99 (60)	1.98 (60)	1.61 (15)	1.60 (30)	1.47 (20)	1.47 (25)
1.84 (70)	1.84 (80)	1.44 (10)	– –	1.43 (25)	1.43 (30)

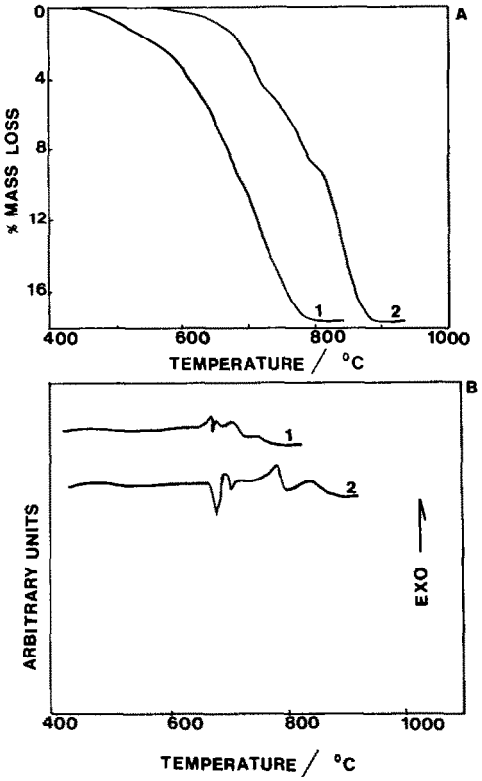

Fig. 3. Thermogravimetric (A) and DTA (B) curves of the reduction of V_2O_5 platelets by CO at different heating rates: curve 1, 5 °C min^{-1}; curve 2, 10 °C min^{-1}.

became visible. X-ray analysis (Table 1) of the reaction products of each of these steps suggested that the reduction reaction can be summarised as follows:

Reaction (1) in the temperature range 550–670 °C

$$3V_2O_5 + 2CO \rightarrow V_6O_{13} + 2CO_2 \quad (1)$$

Reaction (2) in the temperature range 670–705 °C

$$V_6O_{13} + CO \rightarrow 6VO_2 + CO_2 \quad (2)$$

Reaction (3) in the temperature range 705–830 °C

$$2VO_2 + CO \rightarrow V_2O_3 + CO_2 \quad (3)$$

The TG and DTA curves for the reduction of the platelets are given in Fig. 3 which shows that their rate of reduction is slower than that of the powder and is completed at higher temperatures. As a result of these higher temperatures, melting of the V_2O_5 and V_6O_{13} occurs. This gives rise to complicated DTA curves consisting of overlapping melting endotherms and reduction exotherms, see Fig. 3B. As the aim of the study was to obtain experimental data on the reactions which occur in the solid state, it was

therefore decided to concentrate on isothermal techniques below the melting point of V_2O_5.

Isothermal thermal analysis

The isothermal TG curves for the reduction of V_2O_5 powder are shown in Fig. 4A and those of the platelets are in Fig. 4B. The total mass loss obtained corresponded to the formation of V_2O_3 which was confirmed by X-ray powder diffraction as the final product.

In order to follow the reduction process under isothermal conditions, a qualitative X-ray powder diffraction study was employed. The powder was heated under a CO atmosphere in the thermobalance at 550 °C and terminated at certain stages of the reduction. A diffractogram was obtained and the intensity of the main peak of the possible intermediate oxide which can form was plotted as a function of the fractional mass loss. The curve is shown in Fig. 5. The oxide phases which were identified were the same as those formed under dynamic heating conditions. The diagram shows that V_2O_5 and the intermediate oxides are gradually reduced under isothermal conditions. The observed TG curve is therefore a curve which consists of three different overlapping reactions. An increase in the isothermal reduction temperature led to an increase in the rate of the reduction of the

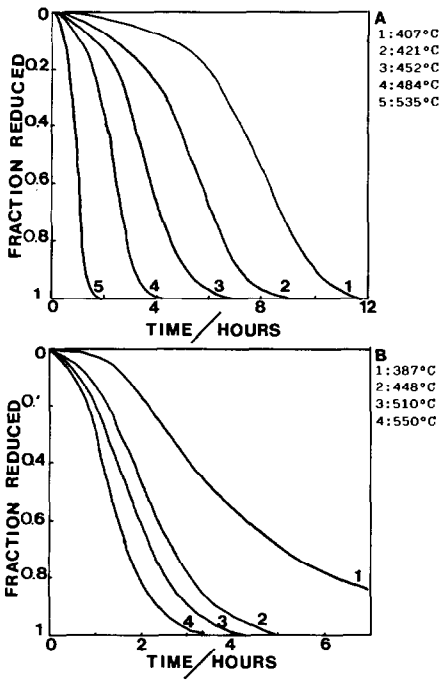

Fig. 4. Isothermal TG reduction curves for V_2O_5 powder (A) and platelets (B).

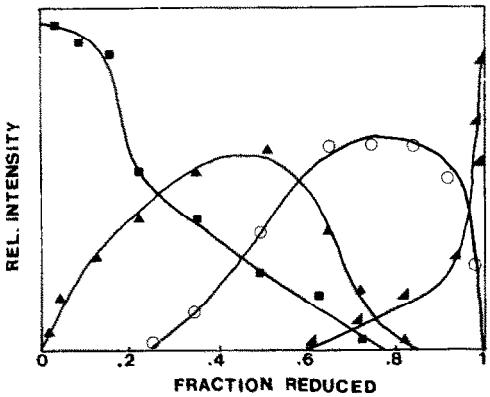

Fig. 5. Formation of various vanadium oxides during the isothermal reduction process: ■, V_2O_5; ▲, V_6O_{13}; ○, VO_2; ◢, V_2O_3.

powder. However, as the temperature is raised, the rate of reduction of the platelets seems to reach a maximum at 460 °C. This effect is clearly illustrated in Fig. 6 which is a plot of the time taken to reach 90% reduction as a function of the isothermal temperature.

Kinetic analysis of the reduction reaction

The isothermal rate data collected between 407 and 575 °C fitted the Avrami–Erofe'ev nucleation and growth model, $[-\ln(1-\alpha)]^{1/n} = k(t-t_0)$, t_0 being the induction period. The value of n was determined as 4. An apparent activation energy of 64.5 kJ mol^{-1} and an ln A (s^{-1}) value of 2.7 were calculated from the Arrhenius plot, Fig. 7A. It is clear from the plot that below 450 °C ($1/T = 1.38 \times 10^{-3}$), a scattering of the points occurs.

The isothermal rate data which were collected between 386 and 596 °C for the platelets seems to fit the equation $[-\ln(1-\alpha)]^{1/2} = k(t-t_0)$. It was,

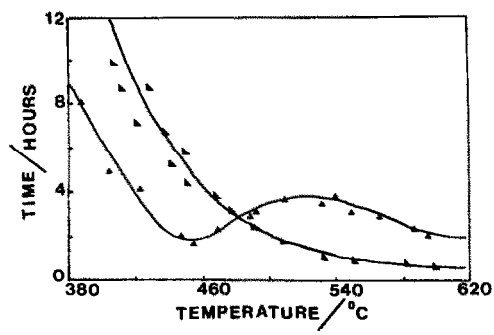

Fig. 6. Reduction time versus isothermal reduction temperature of V_2O_5 powder (◣) and platelets (▲).

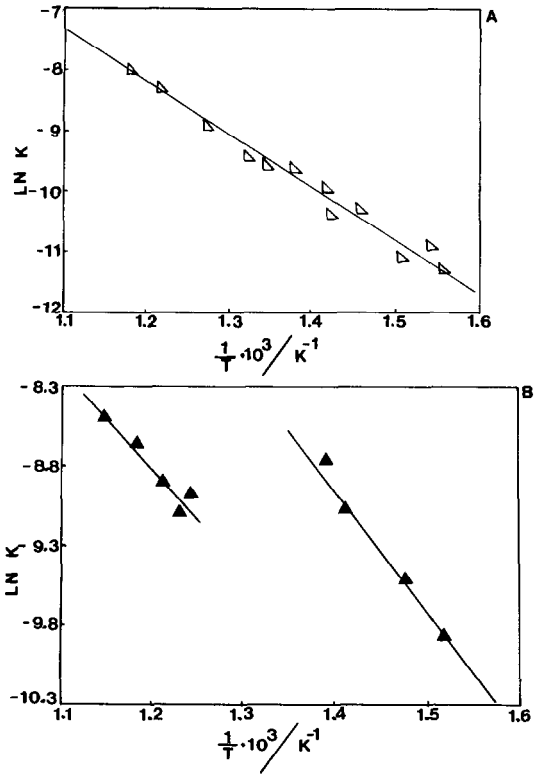

Fig. 7. Arrhenius plots for the reduction of V_2O_5 powder (A) and platelets (B).

however, noticeable that although this model seems to describe the rate data the best below 460 °C, poor linear correlations were obtained. The Arrhenius plot, Fig. 7B, shows two straight lines, one for the data above 500 °C, from which an apparent activation energy of 51.9 kJ mol^{-1} and an ln A (s^{-1}) of 0.26 were calculated, and one below 460 °C from which were calculated $E_a = 64.2$ kJ mol^{-1} and ln A (s^{-1}) = 6.48. This seems to suggest that a change in the mechanism occurs as the temperature is increased. This change in mechanism seems to change the value of the frequency factor rather than the activation energy. This is in agreement with the observation that the reduction rate passes through a maximum at 460 °C as illustrated above.

Partly reduced crystals were investigated using optical and scanning electron microscopy in an effort to give a better description of the geometrical mechanism. Crystals which were heated between 300 and 350 °C were examined under an optical and scanning electron microscope. At this temperature no mass loss was recorded on the thermobalance. The photographs of the crystals, Fig. 8, show that a slight darkening of the crystals has occurred along steps, kinks and dislocations on the (010) crystal plane. SEM studies of the (010) crystal plane indicated the presence of the structures shown in Fig. 9. These structures represent an advanced stage of nuclei

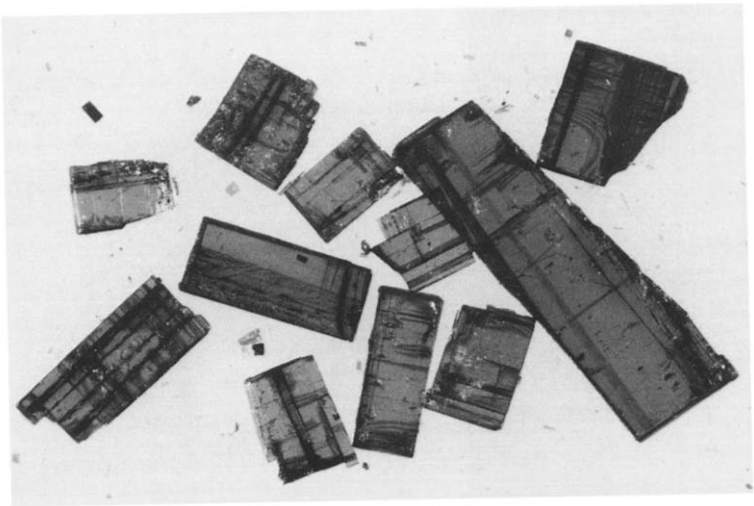

Fig. 8. Photograph showing the crystals heated in CO between 300 and 350 °C in a thermobalance.

formation and growth with the formation of cracks due to shear and lattice collapse. This proves that reduction starts at temperatures below 350 °C although it is not visible on the TG curves. The induction period, as determined from the isothermal curve, is therefore under suspicion but should not influence the value of n or k in the Avrami–Erofe'ev equation.

The micrograph in Fig. 10 represents a cross section of a partly reduced crystal ($\alpha = 0.5$) at 550 °C. It shows that reduction starts on all available surfaces, including those caused by cracking during the nucleation process,

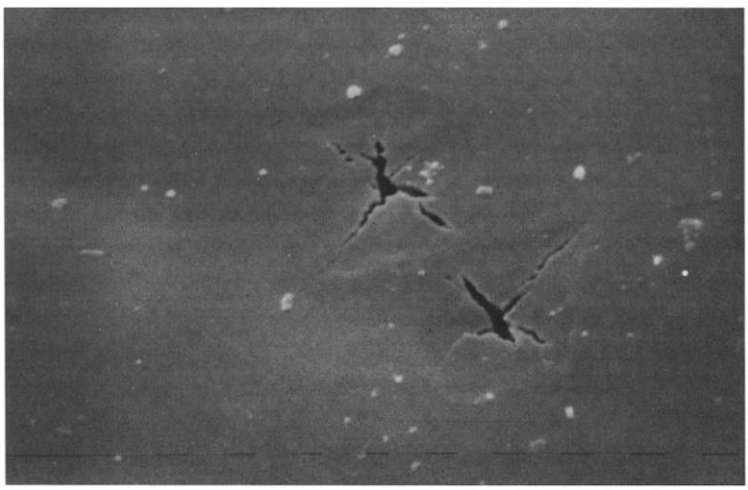

Fig. 9. SEM photograph of crystals heated in CO between 300 and 350 °C in a thermobalance.

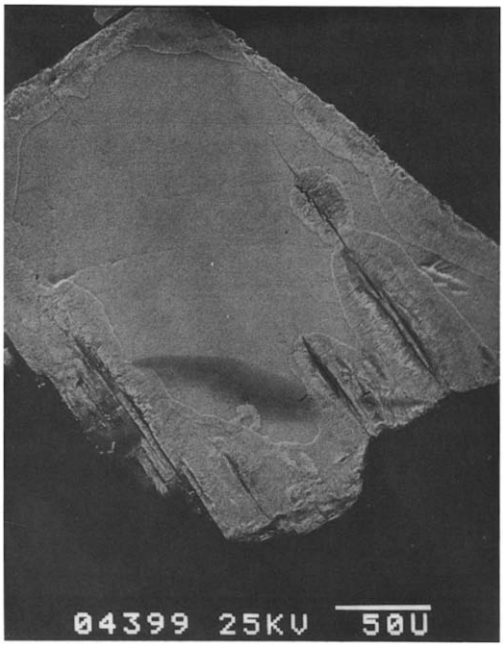

Fig. 10. SEM photograph of partly reduced V_2O_5 crystal.

and then moves inwards towards the centre of the crystal. It can therefore be expected that an oxygen gradient would exist between the centre of the crystal, the unreacted zone, and the surface where reduction had taken place. This implies a movement of oxygen ions from the centre of the crystal towards the surface.

It is, however, not possible at this stage to give a more detailed explanation of the mechanism. More microscopy and other complementary experimental data are needed before this can be done.

ACKNOWLEDGEMENTS

The authors thank the University of Pretoria, the Council for Mineral Technology and the Foundation for Research and Development for financial assistance.

REFERENCES

1 A. Andersson, J. Catal., 76 (1982) 144.
2 M. Inomata, A. Miyamoto and Y. Murakami, J. Catal., 62 (1980) 140.
3 A. Miyamoto, K. Kobayashi, M. Inomata and Y. Murakami, J. Phys. Chem., 86 (1982) 2945.

4 J. Stringer, J. Less-Common Met., 8 (1965) 1.
5 M. Pospisil, J. Therm. Anal., 27 (1983) 77.
6 H. Bosch, B.J. Kip, J.G. van Ommen and P.J. Gellings, J. Chem. Soc., Faraday Trans. I, 80 (1984) 2479.
7 C.P.J. van Vuuren and C.A. Strydom, Inorg. Chem. Acta, 117 (1986) 83.
8 L.A. Jacobs, C.P.J. van Vuuren and P.H. van Rooyen, S. Afr. J. Chem., 39 (1986) 174.